

Article

Rapid Estimation of Static Capacity Based on Machine Learning: A Time-Efficient Approach

Younggill Son ¹ and Woongchul Choi ^{2,*}

¹ Graduate School of Automotive Engineering, Kookmin University, Seoul 02707, Republic of Korea; younggill@kookmin.ac.kr

² Department of Automotive Engineering, Kookmin University, Seoul 02707, Republic of Korea

* Correspondence: danchoi@kookmin.ac.kr

Abstract: With the global surge in electric vehicle (EV) deployment, driven by enhanced environmental regulations and efforts to reduce transportation-related greenhouse gas emissions, managing the life cycle of Li-ion batteries becomes more critical than ever. A crucial step for battery reuse or recycling is the precise estimation of static capacity at retirement. Traditional methods are time-consuming, often taking several hours. To address this issue, a machine learning-based approach is introduced to estimate the static capacity of retired batteries rapidly and accurately. Partial discharge data at a 1 C rate over durations of 6, 3, and 1 min were analyzed using a machine learning algorithm that effectively handles temporally evolving data. The estimation performance of the methodology was evaluated using the mean absolute error (MAE), mean squared error (MSE), and root mean squared error (RMSE). The results showed reliable and fairly accurate estimation performance, even with data from shorter partial discharge durations. For the one-minute discharge data, the maximum RMSE was 2.525%, the minimum was 1.239%, and the average error was 1.661%. These findings indicate the successful implementation of rapidly assessing the static capacity of EV batteries with minimal error, potentially revitalizing the retired battery recycling industry.

Keywords: retired lithium-ion battery; reuse; static capacity; machine learning; rapid estimation



Citation: Son, Y.; Choi, W. Rapid Estimation of Static Capacity Based on Machine Learning: A Time-Efficient Approach. *Batteries* **2024**, *10*, 191. <https://doi.org/10.3390/batteries10060191>

Academic Editors: Seiji Kumagai, Xuan Zhou and Rongheng Li

Received: 3 March 2024

Revised: 20 May 2024

Accepted: 29 May 2024

Published: 31 May 2024



Copyright: © 2024 by the authors. Licensee MDPI, Basel, Switzerland. This article is an open access article distributed under the terms and conditions of the Creative Commons Attribution (CC BY) license (<https://creativecommons.org/licenses/by/4.0/>).

1. Introduction

The rapid increase in the use of electric vehicles (EVs) is contributing to significant reductions in greenhouse gas emissions from transportation systems that used to depend only on an internal combustion engine (IC), which accounts for about 20% of global emissions [1]. This increase in EV usage has caused significant growth in the lithium-ion (Li-ion) battery market. However, this growth is also bringing about inevitable challenges related to the disposal of used Li-ion batteries after their initial application in EVs [2,3]. The retired batteries referred to here include those that have decreased to 80% or less of their initial capacity, those with a long service life, or those that have been replaced due to a sudden accident [4]. Recent studies estimate that the number of retired batteries generated from electric vehicles will increase dramatically after 2030 [5]. Finding ways to recycle electric vehicle batteries that have reached the end of their life and ways to reuse the static capacity of retired batteries has now become a necessity rather than an option. This is important for sustainable resource management and environmental protection. To achieve the above objectives, it is very important to accurately and quickly estimate the static capacity of batteries from electric vehicles after their initial use to make decisions between recycling and reusing, i.e., remanufacturing [6]. A lot of research has been carried out for this purpose [7–10].

1.1. A Review of SOH Estimation Method for Li-Ion Batteries

A battery's static capacity or health status is called its state of health (SOH), which can be defined as a performance measure in terms of the power and energy that the battery can

deliver relative to its original capacity [9]. One of the SOH definitions can be expressed as shown in Equation (1).

$$\text{SOH}(\%) = \frac{\text{Remaining capacity of the battery}}{\text{Nominal capacity of the battery}} \times 100 \quad (1)$$

In previous studies, various methodologies have been employed to estimate a battery's SOH. These methods include direct measurements of voltage, current, and temperature; filter-based estimation; and electrochemical model estimation. The method of directly measuring data such as the voltage, current, etc., of a battery has the advantage of high estimation accuracy for the SOH because it directly measures the real-time changing data of the battery. This method is also useful for battery management because it can monitor the state of the battery in real time [11,12]. However, to estimate the SOH using data directly measured from the battery, it is necessary to develop algorithms accordingly. One disadvantage is that the accuracy of SOH estimation may decrease depending on the precision of the measurement equipment or the error of the sensor [13,14]. Filter-based estimation methods offer several advantages. They can enhance the accuracy of SOH estimation by accounting for the nonlinearity of the battery model. They can estimate the SOH in real time in both online and offline environments. Additionally, they are highly adaptable, as they can reflect the changes in characteristics as the battery ages [15]. However, this approach is subject to the limitation that the process of linearizing the nonlinearity of the battery may introduce errors, and it also has difficulties in modeling the complex chemical structure of the battery [16,17].

To compensate for these drawbacks and to achieve fast and accurate estimation, recent research has adopted machine learning techniques, also known as data-driven methods [18–20]. This approach paves the way for directly processing traditional data streams to estimate the target value faster and with higher accuracy. These machine learning-based methods also leverage data on battery aging characteristics to develop estimation models for the SOH, assembling extensive datasets (such as current, voltage, resistance) for training and evaluation and utilizing various machine learning algorithms for estimation. While it has the disadvantage of requiring a significant amount of training data to improve estimation accuracy, this approach offers the advantage of adaptable SOH estimation under different environmental conditions and operational scenarios [21–24].

Conventionally, methods for diagnosing the static capacity of Li-ion batteries include full charge/discharge/pulse discharge, the internal resistance measurement method, and the EIS (electrochemical impedance spectroscopy) measurement method [25]. Particularly in Korea, a low-current (i.e., 0.1 to 0.3 C) full discharge method is used to diagnose batteries with high precision following the Korea Battery Industry Association standard. Although they have the advantage of being able to measure static capacity with high precision, using these traditional methods is time-consuming and increases the financial burden. Methods for accurately diagnosing the static capacity of retired batteries have been developed with varying degrees of accuracy but typically require significant time for data processing and capacity estimation [26]. If conventional methods are used for the evaluation of retired batteries, it seems obvious that the bottleneck of the long processing time would result in significant economic and environmental losses [6].

Although numerous researchers have successfully addressed the challenge of estimating the static capacity of a battery, few studies have been conducted on diagnosing it rapidly. While deep learning methods have demonstrated promising results in estimating the static capacity of batteries, these machine learning estimation methods are typically studied in isolation, making it challenging to discern their relative strengths and weaknesses [23]. In this study, we developed a methodology to estimate the static capacity of lithium-ion batteries using a machine learning-based model. This model differs from other studies in that it employed 1 min partial discharge data at a 1 C rate to estimate a battery's capacity in a rapid and precise manner. Furthermore, this study differs from previous studies in that it designed its own experiments and conducted experimental validation using the

data, in contrast to other studies that demonstrate comparable performance by utilizing publicly available experimental datasets from NASA or Oxford to assess battery health status [27,28].

This study aimed to diagnose the static capacity of aging batteries rapidly and accurately in electric vehicles. Time series data of cylindrical lithium-ion batteries in various stages of degradation were analyzed to estimate the static capacity of the batteries after use using a recurrent neural network (RNN)-based model. This fast diagnostic method has the advantage of quickly assessing the reusability of batteries, which can reduce the economic costs incurred in the reuse and recycling processes and create a more competitive industrial structure. Consequently, this study presented a methodology that can significantly enhance the industrial and economic benefits associated with the diagnosis of end-of-life batteries in electric vehicles.

1.2. Structure of the Paper

The structure of this paper is organized as follows: Section 1 describes the research background and the necessity, objectives, and outcomes of this study. Section 2 details the experimental setup and methods, along with the specifications of the equipment used to acquire input parameters for battery static capacity estimation. Section 3 discusses the algorithm used in this study, an RNN-based model. Section 4 analyzes the results of the battery static capacity estimation algorithm when utilizing input parameters measured through various experiments. Section 5 provides the conclusion of the current study and summarizes the limitations of the study and future work.

2. Experimental Setup and Methodology

2.1. Experimental Configuration

In this study, data from cylindrical Li-ion batteries, typically found in electric vehicle applications, were used for the analysis with machine learning algorithms. The batteries used in the experiments were NMC (Nickel Manganese Cobalt) series Li-ion batteries and, more specifically, the 'INR21700-40T' model shown in Figure 1a. A picture of the experimental equipment used in the current study is also provided in Figure 1b. The specifications of the battery samples used in the experiments are summarized in Table 1, and the specifications of the experimental equipment, i.e., a cylindrical battery cycler, are also supplied in Table 2.



Figure 1. Experimental setup. (a) Tested cell: INR21700-40T; (b) cylindrical cell cycler.

In the current research, the experiments were conducted mainly in two parts. The first part was to measure transient voltage data during a specified discharge time period. During this measurement part, the direct current internal resistance (DCIR) was acquired after standard charging, and, after that, discharge characteristic data, i.e., the transient voltage response, were measured after a prescribed resting period to ensure electrochemical stability [29]. The second part was to age battery cells intentionally for a prescribed number of cycles. The aging was performed for 100 cycles with constant-current charging and

discharging at a rate of 2 C. A flowchart to describe the experimental sequence is provided in Figure 2, and it shows a subsequence to acquire the transient voltage response and to measure the static capacity of the batteries in their corresponding aging state, aiming to correlate the transient voltage response data with the static capacity data in the respective aging state.

Table 1. Specifications of batteries used in the experiments.

Parameter	Value	Unit
Nominal capacity	4000	mAh
Charging cut-off voltage	4.2 ± 0.05	V
Nominal voltage	3.6	V
Discharging cut-off voltage	2.5	V
Cell weight	70.0	g

Table 2. Specifications of battery charge/discharge equipment, APC-5V20A battery cycler.

Category	Specification	Unit
Rated voltage	0~5	V
Rated current	20/each channel (40 CH)	A
Data processing	10	ms
Accuracy	Full Scale ± 0.05 Voltage, Current Power	%
	Full Scale ± 0.1	
	Full Scale ± 0.2	

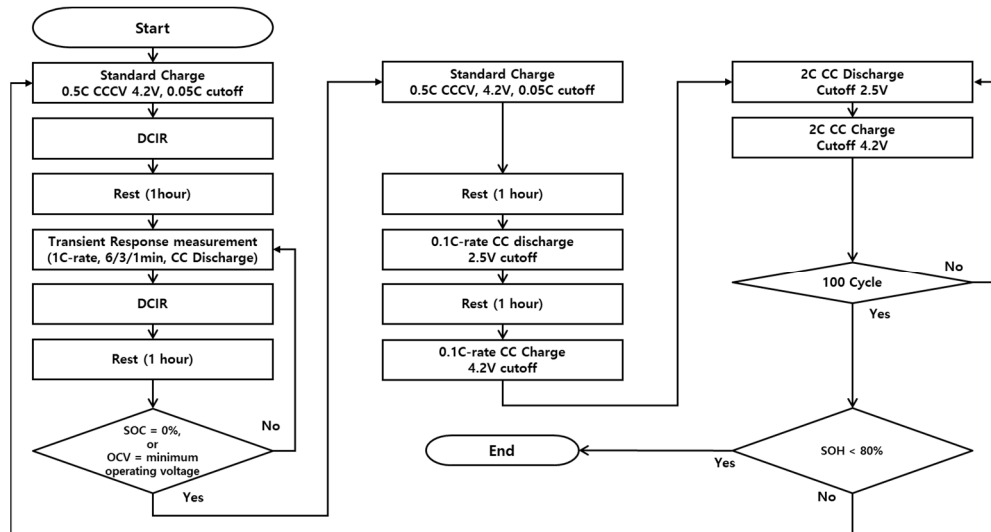


Figure 2. Flowchart of the experiments.

As the main goal of this study was to reduce the estimation time for the battery's static capacity, parametric experiments were carried out for the cases of a 6 min, 3 min, and 1 min discharge period, respectively. In earlier research, training data were collected through constant-current discharging at a rate of 1 C, and the researchers of that study employed a linear regression to assess the static capacity of batteries with the data obtained through partial discharging at 10% state of charge (SOC) intervals [30]. A 10% SOC interval was implemented with a 6 min partial discharge at a 1 C rate, and by utilizing voltage characteristic data, the method effectively used the voltage data at various SOCs to take aging into account for the successful estimation of the static capacities. In order to highlight the current parametric experimental study, partial discharge characteristic data were obtained at a 100% SOC down to a 0% SOC at a 1 C rate for 6 min, 3 min, and 1 min intervals. When discharging for 6 min using a constant-current 1 C rate, 10 steps

of discharging were performed, which means the amount of 10% SOC discharge using a Coulomb counting method during 3 min and 1 min of discharging represented SOC changes of 5% and 1.67%, respectively, and 20 steps and 60 steps of discharging, respectively. The coulomb counting is illustrated in Equation (2). After the above process was repeated and the termination condition was reached, the actual static capacity of the battery was measured through a low-current discharge and charging process to measure the static capacity of the battery.

$$\text{SOC}(t) = \text{SOC}(0) - \int_0^t \frac{I(t)}{C_n} dt \quad (2)$$

A total of 15 battery cells (5 for each experimental condition) were used for the experiment to ensure accurate and diverse data collection. The collected data were preprocessed to observe aging characteristics and electrochemical changes to improve the accuracy and relevance of the subsequent machine learning models. The working hours spent on the completion of the experimental sequence shown in Figure 2 are summarized in Table 3. In this study, the experiments were conducted until the static capacity of the batteries decreased to less than 80%. To verify the integrity of the training and validation data, a random sample was drawn from each experiment, and the decreasing trend of static capacity was analyzed. The change in static capacity due to the aging process of randomly selected samples for each experiment is shown in Figure 3. It shows how the static capacity of a battery changes over the aging cycle. It is important to note here that when the battery is discharged using a 1 C-rate current under three different discharge time conditions (6 min, 3 min, and 1 min), there is little difference in the declining trend of the battery's SOH. This consistent result suggests that the battery's static capacity can be effectively estimated simply using one minute of discharge data.

Table 3. Working hours required for data acquisition based on the discharging period.

Experiment Step	1 C 6 min	1 C 3 min	1 C 1 min	Unit
Measurement Step	* TR + DCIR	15	25	Hour
	Static Capacity	25	25	Hour
Aging Step	100	100	100	Hour
Total (100 cycle)	140	150	189	Hour
Total (1000 cycle)	1400	1500	1890	Hour

* TR stands for transient response, which is the step of measuring the partial discharge voltage. Refer to Figure 2 for the experimental process. When aging was implemented using the cylindrical battery '21700-40T', static capacity was measured to be less than 80% after 1000 cycles, and experiments were conducted for up to 1000 cycles.

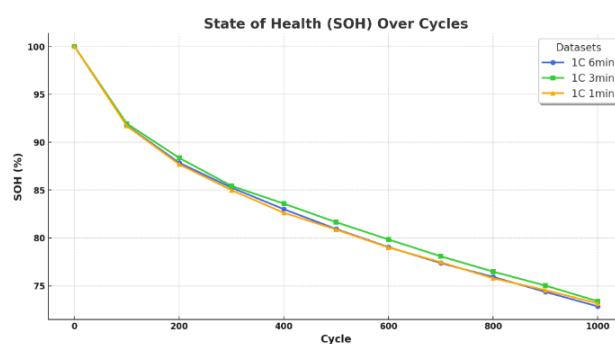


Figure 3. Changes in battery's static capacity along aging cycles.

2.2. Data Analysis

Prior to applying the machine learning scheme, a careful data analysis was carried out with incremental capacity analysis (ICA) and differential voltage analysis (DVA), which

are discussed in a later section, to generate parameters reflecting the aging characteristics of the batteries for further analysis with various machine learning algorithms. Moreover, the analysis utilized the characteristics of the discharge voltage measured after aging, specifically focusing on the voltage response characteristics indicative of aging.

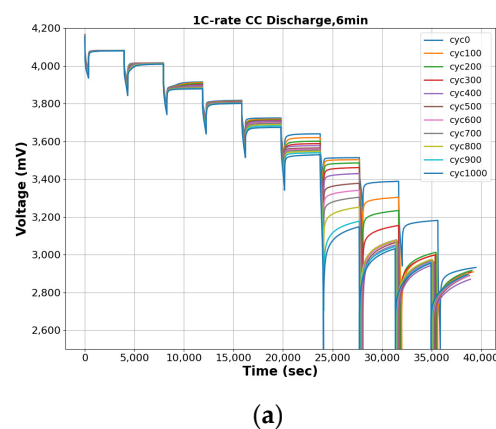
2.2.1. Transient Voltage Response Analysis

In this research, training data for machine learning were obtained through constant-current discharging at a 1 C rate for three different discharging periods, namely 6 min, 3 min, and 1 min, to systematically evaluate the effectiveness among them in an attempt to come up with a faster yet reliable methodology.

Initially, the data obtained through partial discharging for 6 min at a 1 C rate for every 10% SOC were used to link the transient voltage data with the static capacity at the corresponding age through RNN-based machine learning algorithms. The fidelity of the estimation method utilizing an RNN-based machine learning algorithm was verified by separating the learning dataset and the validation dataset completely. After that, the studies were then expanded to include 3 min and 1 min discharges at a 1 C rate. A series of transient discharge voltage graphs at various aging states are illustrated in Figure 4.

Figure 4 illustrates the transient voltage characteristics during the partial discharge interval for each measurement cycle. For the machine learning application, only the transient voltage responses during the partial discharge period, excluding the data from the relaxation period, were employed in the training and validation processes. The transient voltage responses depicted in Figure 5 represent a segment of the voltages obtained during the different partial discharge experiments in Figure 4a–c.

For each experiment, discharge voltage data were measured at every 0.2 s. In other words, for the 6 min discharge period, 1801 voltage data points were acquired during a 10% SOC discharge. For the 3 min discharge, 901 voltage data points were acquired, and for the 1 min discharge, 301 voltage data points were acquired. As the battery aged, the voltage drop became more prominent due to the increase in the internal resistance of the battery cells. This affected the learning and validation data collection in low SOC cases where the transient voltage during discharging at low SOC levels reached the cut-off voltage, limiting the discharge process for safety reasons. As shown in Figure 6a, the numbers of data points acquired during the discharge period decreased as the SOC level decreased in all cases, i.e., for the 6 min, 3 min, and 1 min discharges. An expanded plot of the number of data points acquired for the case of the 1 min discharge is provided for a better understanding of the situation. Therefore, the section of a 30% SOC or less, where the number of data points was lower than that of normal cases, was cut out and not used for machine learning.



(a)

Figure 4. Cont.

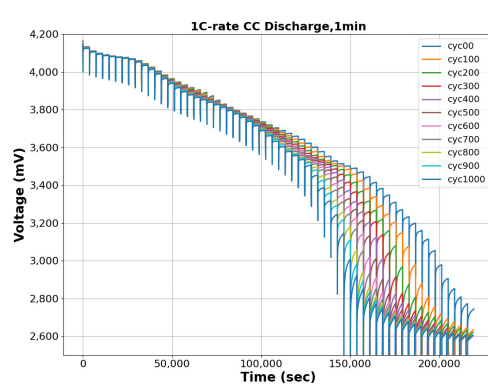
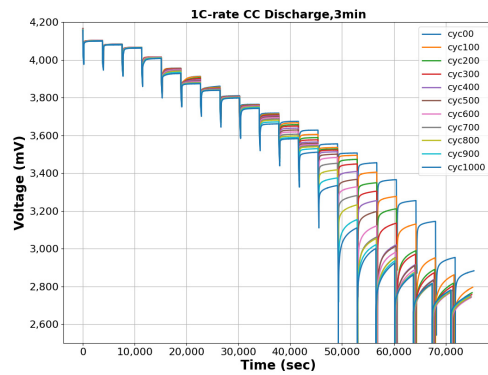


Figure 4. Transient voltage response with different discharge periods. (a) 1 C-rate 6 min discharge; (b) 1 C-rate 3 min discharge; (c) 1 C-rate 1 min discharge.

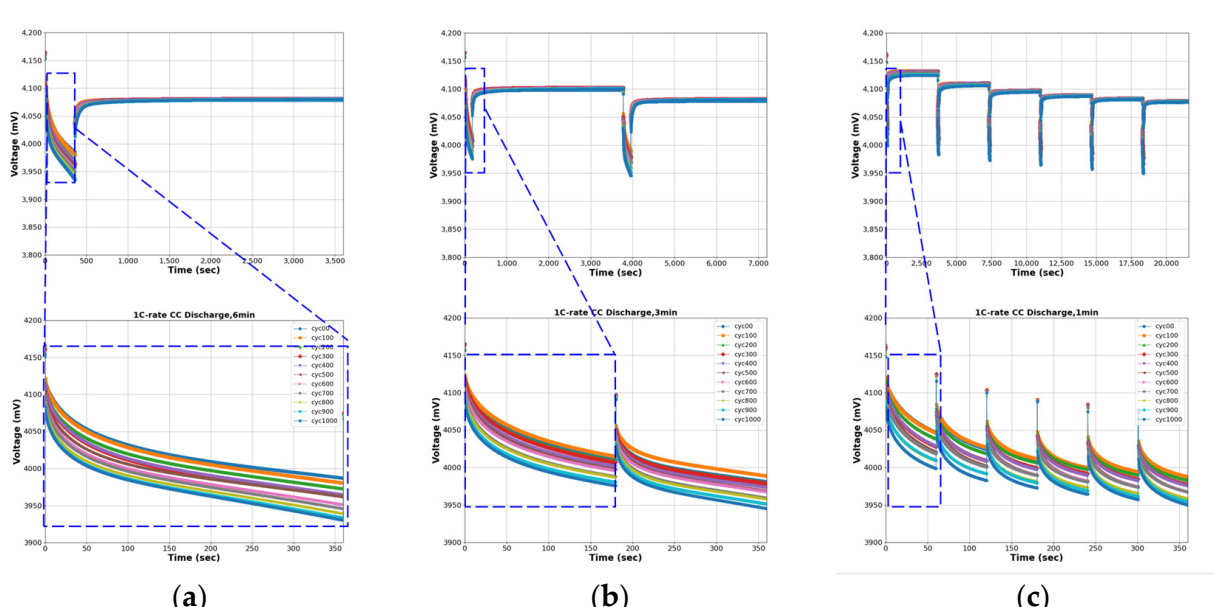


Figure 5. Typical transient voltage responses. (a) 1 C-rate 6 min discharge; (b) 1 C-rate 3 min discharge; (c) 1 C-rate 1 min discharge.

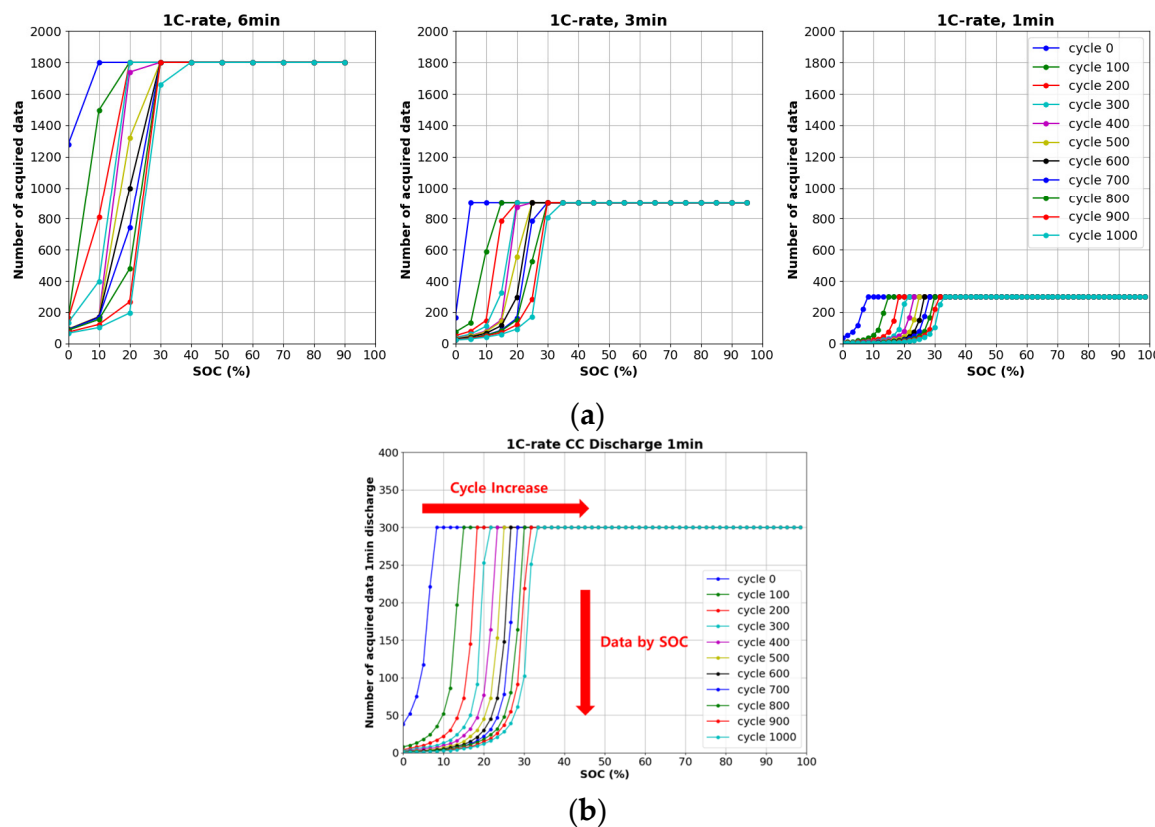


Figure 6. Number of acquired transient voltage data points with aging during partial discharge. (a) Number of acquired data points with aging; (b) number of acquired data points with aging for a 1 min partial discharge.

2.2.2. Incremental Capacity Analysis

Li-ion batteries experience a decrease in electrochemical stability as they age, which can lead to reduced performance and capacity. The decrease in capacity and changes in the voltage drop pattern associated with aging in Li-ion batteries can be analyzed in detail using incremental capacity analysis (ICA). ICA is a method used to non-destructively investigate the capacity state of a battery by tracing the electrochemical characteristics of the cell [31]. It analyzes the changes in a battery's capacity with respect to the battery's voltage over entire or partial cycles. Equation (3) represents the formulas used in the ICA analysis to observe the changes in capacity relative to the changes in voltage. The ICA value is a differential value that represents the relationship between the charge and the voltage. The change in voltage when charging or discharging the battery is measured and displayed on a graph, and then the rate of change in charge at a specific voltage is observed. Through this, the change in charge is observed. The state and progress of internal chemical reactions can be estimated [32]. Through this, the concept of capacity loss in Li-ion batteries can be analyzed by dividing it into the loss of active material (LAM) and the loss of lithium inventory (LLI) [33]. Figure 7 show an ICA performed by organizing the data obtained from this experiment. A graph is shown for the discharge process, with the x-axis representing voltage (V) and the y-axis representing the charge change over the voltage change (dQ/dV). The section where dQ/dV is indicated as a negative number shows that the initial voltage gradually increases due to the electrochemical reaction that occurs in the discharge section, and the electrochemical reaction is maintained stably in the voltage stabilization section (voltage relaxation). The specific peak point during the discharge process varies with aging. During the discharge process, a peak appears as lithium ions are extracted. The reason for

the peak shift with aging is because the internal negative resistance increases due to the increase in the solid electrolyte interphase (SEI) layer with aging.

$$IC = \frac{dQ}{dV} = I \times \frac{dt}{dV} \approx \frac{\Delta Q}{\Delta V} \quad (3)$$

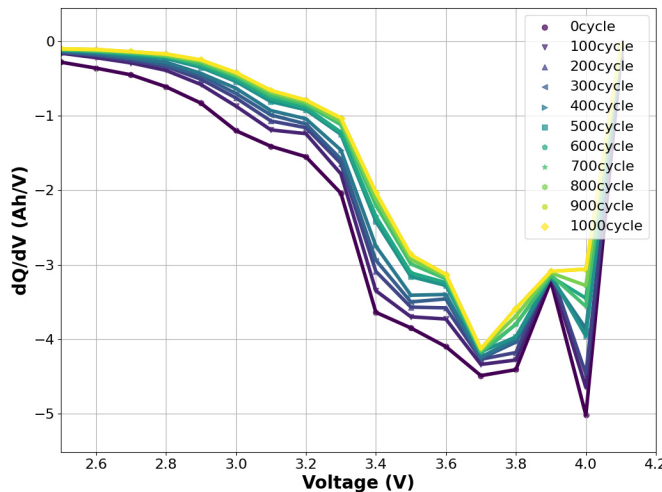


Figure 7. dQ/dV with respect to voltage with aging as a parameter.

2.2.3. Differential Voltage Analysis

The ICA method and the DVA method are the main technologies used to evaluate the health status of Li-ion batteries. The ICA method is used to identify and separate independent components within a battery and has the disadvantage of requiring a large amount of data. On the other hand, the DVA method is used as a method to analyze the voltage change in a battery, determine the imbalance between cells, and evaluate the state of the battery. Figure 8 shows a DVA performed by organizing the data obtained from this experiment. The graph shows the discharge process, with the x-axis representing V and the y-axis representing the voltage change over the charge change (dV/dQ).

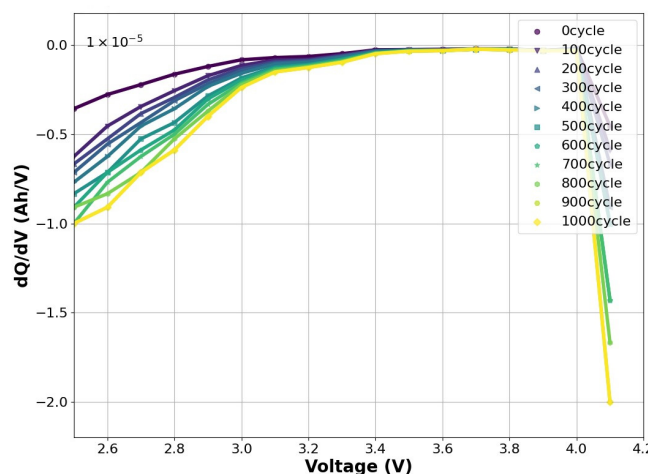


Figure 8. dV/dQ with respect to voltage with aging as a parameter.

DVA is a quantitative method for evaluating the static capacity of a battery. It considers several important parameters related to the battery's capacity, internal resistance, and voltage characteristics. The main parameter is dV/dQ , which shows the voltage change according to the capacity change. It is used in an inverse-function relationship with the ICA method and plays a complementary role. In this study, the ICA method and the DVA

method were used to organize data to be learned for machine learning. The experiment differed from the existing DVA method in that data were acquired through partial discharge at a constant 1 C-rate current. Consequently, the current value was determined to be a fixed value, and the voltage change over time was observed and used as learning data. Equation (4) represents the relationship between the ICA and the DVA and was used as a key parameter for machine learning in this study.

$$IC^{-1} = DVA = I \times \frac{dV}{dt} = \frac{dV}{dQ} \quad (4)$$

The data acquired through the ICA method and the DVA method could be used to observe changes in voltage and capacity due to aging, and therefore, they were selected as input parameters for the machine learning algorithm to estimate the health status of Li-ion batteries. In addition, to improve the performance of the estimation model, additional data that can be acquired during the discharge process were also utilized. Through this process, the model was able to learn the correlation between existing discharge characteristics and the health status of Li-ion batteries.

3. Deep Learning-Based Estimation Methodology

This research examines various methodologies for estimating battery health through the use of electrical and physicochemical measurements, including voltage, current, and temperature. It places a particular emphasis on machine learning and data-driven approaches, with a focus on deep neural network models.

The most prominent deep neural network models include convolutional neural networks (CNNs), recurrent neural networks (RNNs), generative adversarial neural networks (GANs), autoencoders, and perceptrons. In this study, an RNN-based model was employed, which has been demonstrated to be effective for processing time series data. RNNs are particularly well suited for estimating the state of health (SOH) of batteries due to their proficiency in handling time-dependent data. The inherent nature of a battery's SOH, which varies over time, aligns seamlessly with the capabilities of RNNs to effectively learn and carry out estimation from time series data. One of the defining characteristics of RNNs is their memory function, which enables the model to retain and utilize previous state information, thereby facilitating more accurate estimation based on historical data. Moreover, RNNs possess a robust ability to model complex nonlinear relationships, a crucial attribute given that a battery's SOH is influenced by various nonlinear factors [20,22,34]. Collectively, these insights demonstrate the suitability of RNNs for battery SOH estimation. They exploit their strengths in time series data processing, memory utilization, and nonlinear modeling capabilities.

The algorithm utilized in this study employed an RNN-based model, which is effective for processing time series data because it can detect the temporal continuity of voltage response characteristics and electrochemical changes as batteries age. The basic structure of an RNN is depicted in Figure 9. Equations (5) and (6) illustrate the fundamental structure of the RNN depicted in Figure 9. RNNs consist of interconnected layers that facilitate the processing of sequential data over time [35]. At each time step, the input layer receives time series data, such as partial discharge voltages and currents acquired over the aging stages of the battery. These inputs are then processed through recurrent connections, where information from previous time steps is incorporated to generate an output at the current time step. This recurrent nature enables the network to capture temporal dependencies and make estimations based on historical information. Finally, the output layer represents the static capacity of the battery, providing valuable insights into its health and performance.

$$y_t = W_{ay}h_t + b_y \quad (5)$$

$$a_t = \tanh(W_{aa}a_{t-1} + W_{ax}x_t + b_h) \quad (6)$$

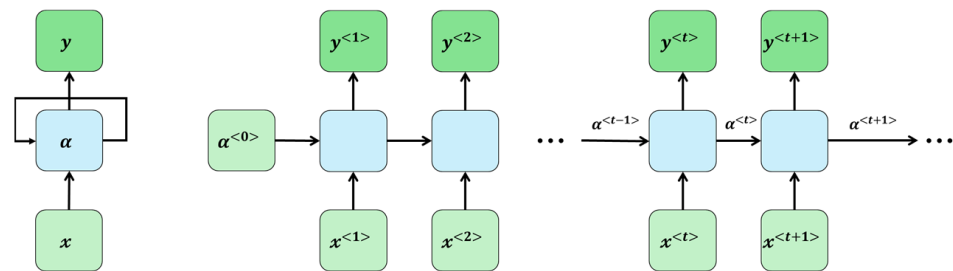


Figure 9. Architecture of an RNN.

The experimental dataset for battery aging was obtained through experimentation, where 15 Li-ion (21,700) cells with a capacity of 4 Ah were cycled at room temperature (RT) to 72% of their nominal capacity. The framework of the learning process consists of several steps: data preprocessing, training, and testing the RNN-based modeling algorithm. The process of deriving estimates using this model is depicted in Figure 10. Following the removal of outliers, the application of min–max normalization, and the division of the data into a training set and a test set, the hyperparameter tuning of the model was initiated. Table 4 presents the parameter tuning of the estimation model. The model was constructed, and the testing environment was configured using MATLAB 2023a.

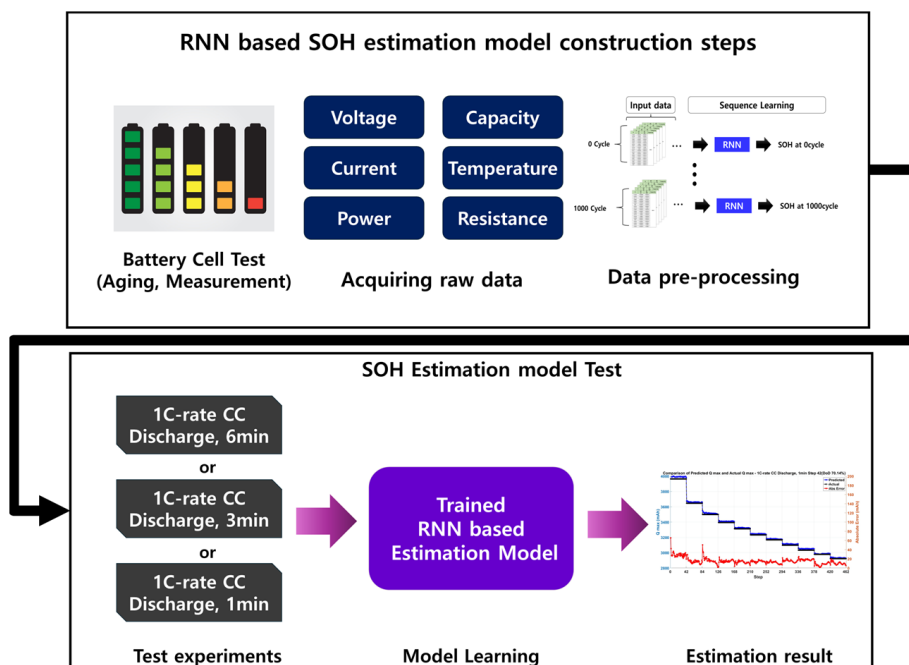


Figure 10. Overall flow chart for the constructed ML model.

Table 4. Parameter settings for the ML-based model.

Parameter	Value Setting
Optimizer	Adam
Learning Rate	0.01
Mini Batch Size	30
Epochs	1500
Dropout Rate	0.1

4. Analysis Results

In order to extract the characteristics of the voltage change over time and parameters that can indicate the relationship between the voltage change and the capacity, the discharge

of CC at a rate of 1 C for various time periods, such as 6 min, 3 min, and 1 min, was performed. These experiments were then used as training data for static capacity diagnosis. For each experiment, five samples were utilized to obtain data, with three of the obtained datasets employed for training the model and the remaining two datasets utilized for validation and testing, respectively. An RNN-based model was employed to estimate the SOH utilizing the acquired data.

For the training data, data from the interval of 100% to 30% SOC, which corresponds to 70% of the depth of discharge (DoD), were used for model training and testing in order to increase the precision of the diagnosis. The evaluation metrics employed to assess the performance of the estimated models were the mean absolute error (MAE), the mean square error (MSE), and root mean square error (RMSE) of each experimental result. These metrics are commonly utilized in machine learning and deep learning. The evaluation methods are defined in Equations (7)–(9).

$$\text{MAE} = \frac{1}{n} \sum_{i=1}^n |Q_{max,predict_i} - Q_{max,real_i}| \quad (7)$$

$$\text{MSE} = \frac{1}{n} \sum_{i=1}^n (Q_{max,predict_i} - Q_{max,real_i})^2 \quad (8)$$

$$\text{RMSE} = \sqrt{\frac{1}{n} \sum_{i=1}^n (Q_{max,predict_i} - Q_{max,real_i})^2} \quad (9)$$

The performance of the ML model was evaluated by comparing the RMSE data based on training data partially discharged for 6 min, 3 min, and 1 min at a 1 C rate. The validation results for each experiment are presented in Table 5.

Table 5. Comparison of various errors from 6 min, 3 min, and 1 min discharge data.

	Value	6 min Data	3 min Data	1 min Data	Unit
MAE	Max	0.03109	0.025189	0.024069	-
	Min	0.010126	0.010138	0.010316	-
	Average	0.018463	0.015386	0.0153181	-
MSE	Max	0.001667	0.0001	0.000637	-
	Min	0.000151	0.000178	0.000153	-
	Average	0.000644	0.000403	0.000283	-
RMSE	Max	4.0816	3.1677	2.5255	%
	Min	1.2289	1.3343	1.2385	%
	Average	2.4909	1.9805	1.6609	%

The MAE values, as shown in Table 5, indicate the average magnitude of the errors between the estimated and actual values. For the 6 min partial discharge data, the maximum error was 0.03109, the minimum error was 0.010126, and the average error was 0.018463. For the three-minute partial discharge data, the maximum error was 0.025189, the minimum error was 0.010138, and the average error was 0.015386. For the one-minute partial discharge data, the maximum error was 0.024069, the minimum error was 0.010316, and the average error was 0.0153181. These results indicate that the model's estimations are more accurate with shorter discharge times, as evidenced by the decreasing average MAE with decreasing discharge duration.

The MSE values, which represent the average of the squared differences between the estimated and actual values, provide insight into the variance of the estimation errors. The MSE values for the 6 min, 3 min, and 1 min partial discharge data were 0.001667, 0.0001, and 0.000637 (max), respectively, with a minimum value of 0.0001. The MSE values for the 51, 0.000178, and 0.000153 (min) datasets were 0.000644, 0.000403, and 0.000283 (average), respectively. The lower mean squared error (MSE) values for the shorter discharge times

indicate that the model exhibits greater consistency in estimation accuracy with more frequent data points.

The RMSE values provide a direct interpretation of the model's estimation error in the same units as the original data. For the 6 min partial discharge data, the maximum RMSE was 4.082%, the minimum RMSE was 1.229%, and the average RMSE was 2.49%. For the three-minute partial discharge data, the maximum RMSE was 3.168%, the minimum RMSE was 1.334%, and the average RMSE was 1.98%. For the one-minute partial discharge data, the maximum RMSE was 2.525%, the minimum RMSE was 1.239%, and the average RMSE was 1.661%.

The results indicate that the error in SOH estimation decreases as the discharge time shortens. This suggests that learning from partial discharge data minimizes gaps in the data, leading to more accurate estimations. To this end, a constant-current discharge at a 1 C rate for 6 min was performed to measure the voltage change corresponding to a 10% reduction in the SOC. The data were trained in 10 steps from 100% to 0% SOC. Furthermore, the voltage response at 5% and 1.67% SOC reductions was obtained from 3 min and 1 min discharges, respectively, allowing for more precise estimates at different SOC stages and enhancing the diagnostic precision of static capacity. To assess the stability of the model and input parameters, various RMSE values obtained through more than 100 iterations are presented in Figure 11, along with the corresponding MAE and MSE values. The analysis confirms that shorter discharge durations result in lower error metrics, thereby highlighting the importance of frequent data collection for accurate SOH estimation.

The results presented in Table 5 and Figure 11 indicate that a single minute of partial discharge transient voltage response data at a 1 C rate is sufficient to provide a reasonably accurate estimate of the capacitance. Figure 12 illustrates the estimated static capacitance of the cell, along with the actual static capacitance values measured in each experiment for the 6, 3, and 1 min discharge periods.

Figure 12 illustrates the capacity value on the y-axis and the number of input data points according to the SOC on the x-axis. Only data up to the 70% DoD bin were utilized for training to enhance diagnostic precision. Consequently, for the 6 min discharge data, seven steps out of a total of ten steps, excluding three steps below 30% SOC, represent the partial discharge bin at 10% SOC reduction. Similarly, for the 3 min and 1-min discharge data, the exclusion of steps below 30% SOC results in the retention of 14 and 42 steps, respectively, out of a total of 20 and 60 steps, respectively. As illustrated in Figure 12, the estimation error in the low SOC bin decreases as the duration of the partial discharge decreases.

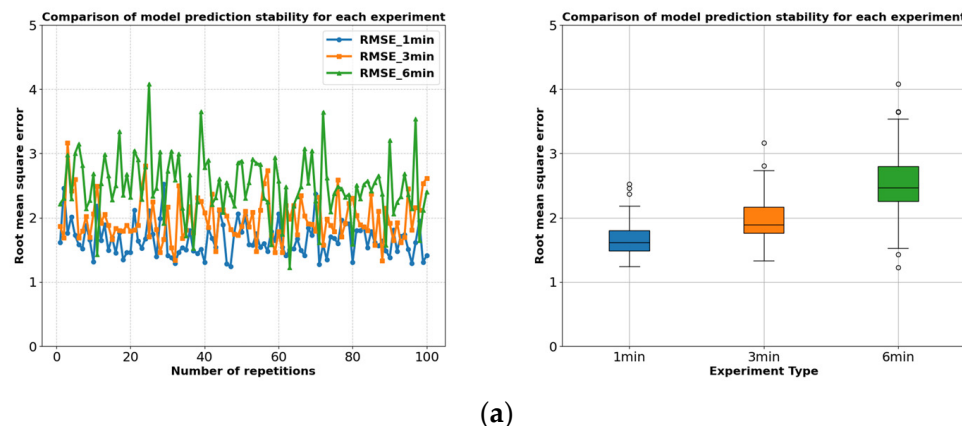


Figure 11. Cont.

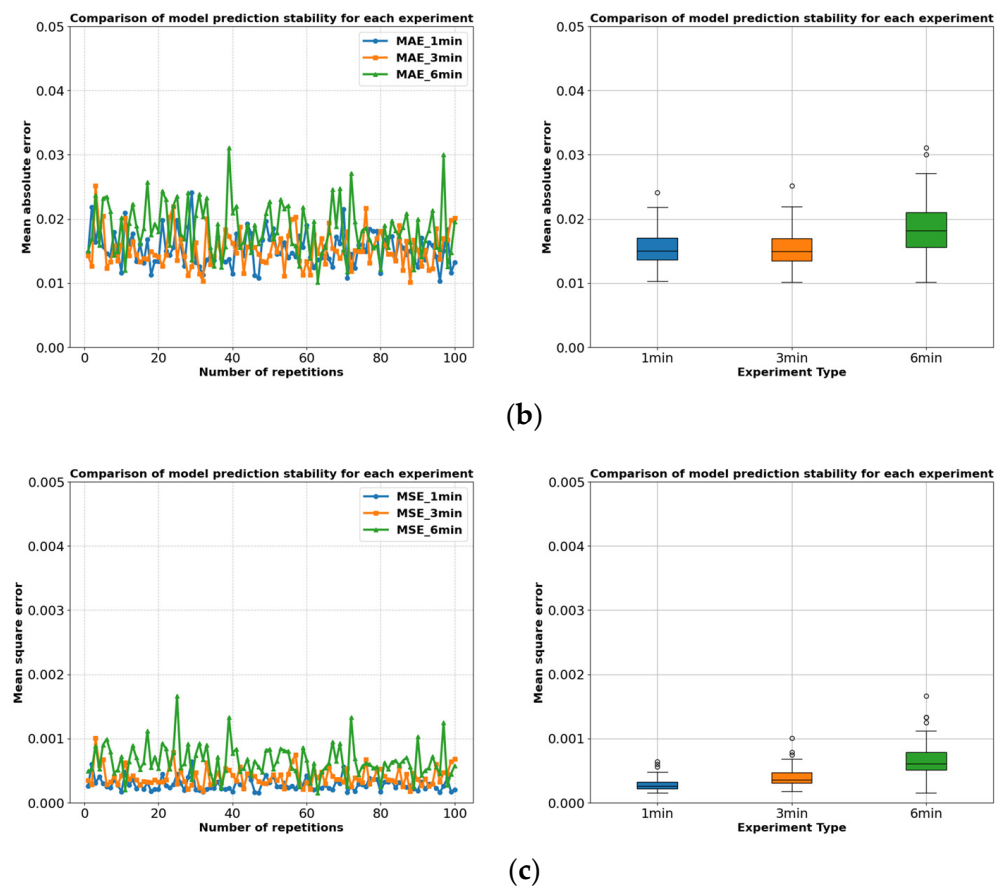


Figure 11. Stability of established models in terms of RMSE, MAE, and MSE. (a) RMSE errors with respect to the number of repetitions for various discharge periods; (b) MAE errors with respect to the number of repetitions for various discharge periods; (c) MSE errors with respect to the number of repetitions for various discharge periods.

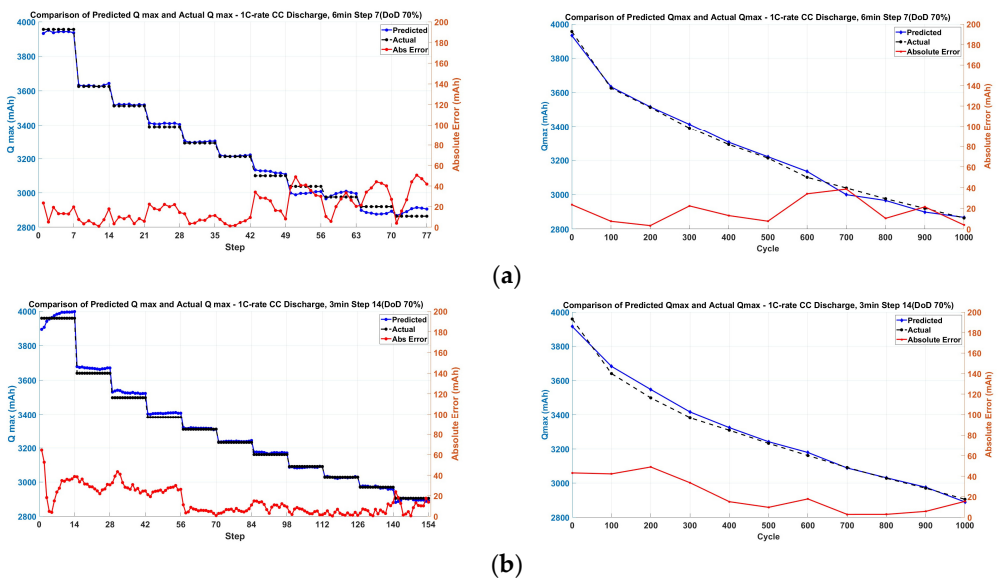


Figure 12. Cont.

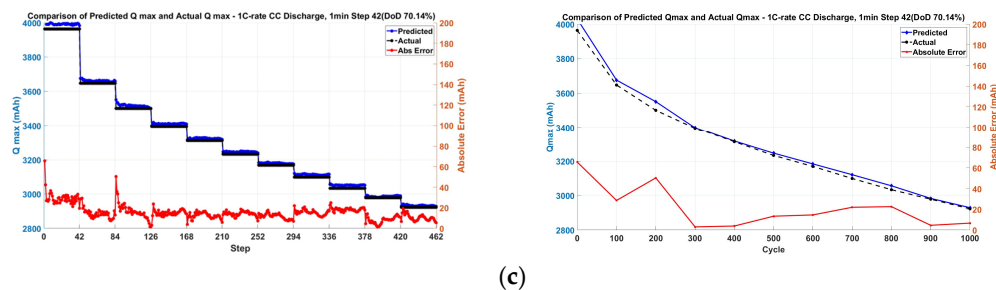


Figure 12. Estimated and actual static capacity and errors for every step and every 100 cycles based on 6 min, 3 min and 1 min discharge data. (a) Estimated and actual static capacity for every step and every 100 cycles based on 6 min discharge data; (b) estimated and actual static capacity for every step and every 100 cycles based on 3 min discharge data; (c) estimated and actual static capacity for every step and every 100 cycles based on 1 min discharge data.

5. Conclusions and Future Study

In order to solve the problems of precision, reliability, and rapidity in estimating the static capacity of lithium-ion batteries, which are mainly used in electric vehicles, this paper proposes a method for diagnosing the static capacity of lithium-ion batteries by learning the time series characteristics of changes in discharge voltage and capacity measured during partial discharge using an RNN-based estimation model. The constant-current partial discharge times at a 1 C rate were set to 6 min, 3 min, and 1 min, respectively, to characterize the voltage change over time and the capacity change with the voltage change as the main parameters that evolve with the aging of lithium-ion batteries. The model was constructed using experimental data from real Li-ion batteries and then verified experimentally. The experimental results showed that the RMSE of the 6 min partial discharge data ranged from 1.229% to 4.082%, with an average RMSE of 2.49%. The RMSE of the 3 min partial discharge data ranged from 1.334% to 3.168%, with an average RMSE of 1.98%. For the 1 min partial discharge data, the RMSE ranged from 1.239% to 2.525%, with an average RMSE of 1.661%. These results show that even with a short partial discharge time, the estimation accuracy of the proposed model was precise and acceptably reliable. By continuously training and developing a model to diagnose the static capacity of batteries using a machine learning-based model that is useful for large-scale data processing, this method is expected to be able to diagnose the static capacity of retired batteries from EVs quickly and accurately for the recycling and reuse industries, thereby increasing the economic value of lithium-ion batteries.

While the current research shows the development of a fast and accurate method for estimating the static capacity of a battery, there are several avenues for further exploration and development.

- (1) Exploration of the applicability of various cell compositions and shapes: Although this paper has focused on 21,700 cylindrical Li-ion batteries, it is necessary to extend the applicability of the proposed method to various shapes of battery cells, such as pouch, prismatic, etc., and cells with various cell performances. Furthermore, it would be interesting to evaluate the impact of different battery rheologies and chemical compositions on the model to expand its applicability at industrial sites.
- (2) Analysis of estimation precision under various temperature conditions considering the use environment of electric vehicles: In this study, experiments and data acquisition were conducted in a room-temperature environment, which is the setting for the actual retired battery treatment process. However, since the distribution and operating environment of electric vehicles represent different environments around the world and aged batteries may have different electrical and electrochemical characteristics under different temperature conditions, it is necessary to conduct experiments and verification considering aged batteries under different temperature conditions to expand and improve the proposed method.

- (3) Practical applications of the proposed method and strategy formulation: The objective of this study is to contribute to the optimization of the battery recycling process and the promotion of sustainable resource utilization. In future research, it is necessary to further investigate the applicability of the research results by formulating strategies for the commercial application of these models to promote practicality throughout the battery reuse industry.

Author Contributions: Conceptualization, W.C.; methodology, W.C.; software, Y.S. and W.C.; validation, Y.S. and W.C.; formal analysis, W.C.; investigation, Y.S. and W.C.; resources, W.C.; data curation, Y.S.; writing—original draft preparation, Y.S.; writing—review and editing, W.C.; visualization, Y.S.; supervision, W.C.; project administration, Y.S.; funding acquisition, W.C. All authors have read and agreed to the published version of the manuscript.

Funding: This work was supported by the Technology Development Program for Automotive Industry (20022377), funded by the Ministry of Trade, Industry and Energy (MOTIE, Republic of Korea).

Data Availability Statement: The data presented in this study are available upon reasonable request from the corresponding author.

Conflicts of Interest: The authors declare no conflicts of interest.

References

1. Mala, P.; Palanivel, M.; Priyan, S.; Anbazhagan, N.; Acharya, S.; Joshi, G.P.; Ryoo, J. Sustainable Decision-Making Approach for Dual-Channel Manufacturing Systems under Space Constraints. *Sustainability* **2021**, *13*, 11456. [[CrossRef](#)]
2. Lee, H.D.; Lim, O.T. Policy Suggestion for Fostering the Industry of Using End of Life EV Batteries. *Trans. Korean Hydrg. New Energy Soc.* **2021**, *32*, 263–270. [[CrossRef](#)]
3. Chen, M.; Ma, X.; Chen, B.; Arsenault, R.; Karlson, P.; Simon, N.; Wang, Y. Recycling end-of-life electric vehicle lithium-ion batteries. *Joule* **2019**, *3*, 2622–2646. [[CrossRef](#)]
4. Yao, L.; Xu, S.; Tang, A.; Zhou, F.; Hou, J.; Xiao, Y.; Fu, Z. A review of lithium-ion battery state of health estimation and prediction methods. *World Electr. Veh. J.* **2021**, *12*, 113. [[CrossRef](#)]
5. Harper, G.; Sommerville, R.; Kendrick, E.; Driscoll, L.; Slater, P.; Stolkin, R.; Walton, A.; Christensen, P.; Heidrich, O.; Lambert, S.; et al. Recycling lithium-ion batteries from electric vehicles. *Nature* **2019**, *575*, 75–86. [[CrossRef](#)] [[PubMed](#)]
6. Meng, K.; Xu, G.; Peng, X.; Youcef-Toumi, K.; Li, J. Intelligent disassembly of electric-vehicle batteries: A forward-looking overview. *Resour. Conserv. Recycl.* **2022**, *182*, 106207. [[CrossRef](#)]
7. Das, K.; Kumar, R. Electric vehicle battery capacity degradation and health estimation using machine-learning techniques: A review. *Clean Energy* **2023**, *7*, 1268–1281. [[CrossRef](#)]
8. Basia, A.; Simeu-Abazi, Z.; Gascard, E.; Zwolinski, P. Review on State of Health estimation methodologies for lithium-ion batteries in the context of circular economy. *CIRP J. Manuf. Sci. Technol.* **2021**, *32*, 517–528. [[CrossRef](#)]
9. Weng, C.; Cui, Y.; Sun, J.; Peng, H. On-board state of health monitoring of lithium-ion batteries using incremental capacity analysis with support vector regression. *J. Power Sources* **2013**, *235*, 36–44. [[CrossRef](#)]
10. Anekal, L.; Samanta, A.; Williamson, S. Wide-ranging parameter extraction of Lithium-ion Batteries to Estimate State of Health using Electrochemical Impedance Spectroscopy. In Proceedings of the 2022 IEEE 1st Industrial Electronics Society Annual On-Line Conference (ONCON), Kharagpur, India, 9–11 December 2022; IEEE: Piscataway, NJ, USA, 2022.
11. Zou, Y.; Hu, X.; Ma, H.; Li, S.E. Combined state of charge and state of health estimation over lithium-ion battery cell cycle lifespan for electric vehicles. *J. Power Sources* **2015**, *273*, 793–803. [[CrossRef](#)]
12. Wang, Z.; Zhao, X.; Fu, L.; Zhen, D.; Gu, F.; Ball, A.D. A review on rapid state of health estimation of lithium-ion batteries in electric vehicles. *Sustain. Energy Technol. Assess.* **2023**, *60*, 103457. [[CrossRef](#)]
13. Lin, C.; Tang, A.; Wang, W. A review of SOH estimation methods in Lithium-ion batteries for electric vehicle applications. *Energy Procedia* **2015**, *75*, 1920–1925. [[CrossRef](#)]
14. Hong, S.; Kang, M.; Jeong, H.; Baek, J. State of health estimation for lithium-ion batteries using long-term recurrent convolutional network. In Proceedings of the IECON 2020 the 46th Annual Conference of the IEEE Industrial Electronics Society, Singapore, 18–21 October 2020; IEEE: Piscataway, NJ, USA, 2020.
15. Tan, X.; Tan, Y.; Zhan, D.; Yu, Z.; Fan, Y.; Qiu, J.; Li, J. Real-time state-of-health estimation of lithium-ion batteries based on the equivalent internal resistance. *IEEE Access* **2020**, *8*, 56811–56822. [[CrossRef](#)]
16. Cui, Z.; Hu, W.; Zhang, G.; Zhang, Z.; Chen, Z. An extended Kalman filter based SOC estimation method for Li-ion battery. *Energy Rep.* **2022**, *8*, 81–87. [[CrossRef](#)]
17. Xie, J.; Wei, X.; Bo, X.; Zhang, P.; Chen, P.; Hao, W.; Yuan, M. State of charge estimation of lithium-ion battery based on extended Kalman filter algorithm. *Front. Energy Res.* **2023**, *11*, 1180881. [[CrossRef](#)]

18. Fei, Z.; Zhang, Z.; Yang, F.; Tsui, K.-L. Deep learning powered rapid lifetime classification of lithium-ion batteries. *eTransportation* **2023**, *18*, 100286. [[CrossRef](#)]
19. Lin, Y.H.; Ruan, S.J.; Chen, Y.X.; Li, Y.F. Physics-informed deep learning for lithium-ion battery diagnostics using electrochemical impedance spectroscopy. *Renew. Sustain. Energy Rev.* **2023**, *188*, 113807. [[CrossRef](#)]
20. Chemali, E.; Kollmeyer, P.J.; Preindl, M.; Fahmy, Y.; Emadi, A. A convolutional neural network approach for estimation of li-ion battery state of health from charge profiles. *Energies* **2022**, *15*, 1185. [[CrossRef](#)]
21. Shu, X.; Shen, S.; Shen, J.; Zhang, Y.; Li, G.; Chen, Z.; Liu, Y. State of health prediction of lithium-ion batteries based on machine learning: Advances and perspectives. *iScience* **2021**, *24*, 103265. [[CrossRef](#)]
22. Tian, J.; Xiong, R.; Shen, W.; Lu, J.; Yang, X.-G. Deep neural network battery charging curve prediction using 30 points collected in 10 min. *Joule* **2021**, *5*, 1521–1534. [[CrossRef](#)]
23. Guo, S.; Ma, L. A comparative study of different deep learning algorithms for lithium-ion batteries on state-of-charge estimation. *Energy* **2023**, *263*, 125872. [[CrossRef](#)]
24. Gou, B.; Xu, Y.; Feng, X. An ensemble learning-based data-driven method for online state-of-health estimation of lithium-ion batteries. *IEEE Trans. Transp. Electrif.* **2020**, *7*, 422–436. [[CrossRef](#)]
25. Mussi, M.; Pellegrino, L.; Restelli, M.; Trovò, F. An online state of health estimation method for lithium-ion batteries based on time partitioning and data-driven model identification. *J. Energy Storage* **2022**, *55*, 105467. [[CrossRef](#)]
26. Berecibar, M.; Gandiaga, I.; Villarreal, I.; Omar, N.; Van Mierlo, J.; van den Bossche, P. Critical review of state of health estimation methods of Li-ion batteries for real applications. *Renew. Sustain. Energy Rev.* **2016**, *56*, 572–587. [[CrossRef](#)]
27. Du, C.; Tian, J.; Xiong, R.; Wang, Y.; Zhang, Q.; Li, F. Research on state-of-health estimation for lithium-ion batteries based on the charging phase. *Energies* **2023**, *16*, 1420. [[CrossRef](#)]
28. Huang, K.; Zhang, Z.; Li, M.; Wang, H.; Chen, X.; Zhang, Y. State of health estimation of lithium-ion batteries based on fine-tuning or rebuilding transfer learning strategies combined with new features mining. *Energy* **2023**, *282*, 128739. [[CrossRef](#)]
29. Laschuk, N.O.; Easton, E.B.; Zenkina, O.V. Reducing the resistance for the use of electrochemical impedance spectroscopy analysis in materials chemistry. *RSC Adv.* **2021**, *11*, 27925–27936. [[CrossRef](#)] [[PubMed](#)]
30. Jung, C.; Choi, W. Rapid Estimation of Battery Storage Capacity through Multiple Linear Regression. *Batteries* **2023**, *9*, 424. [[CrossRef](#)]
31. Dubarry, M.; Anseán, D. Best practices for incremental capacity analysis. *Front. Energy Res.* **2022**, *10*, 1023555. [[CrossRef](#)]
32. Kalogiannis, T.; Stroe, D.I.; Nyborg, J.; Nørregaard, K.; Christensen, A.E.; Schaltz, E. Incremental capacity analysis of a lithium-ion battery pack for different charging rates. *ECS Trans.* **2017**, *77*, 403. [[CrossRef](#)]
33. Birkl, C.R.; Roberts, M.R.; McTurk, E.; Bruce, P.G.; Howey, D.A. Degradation diagnostics for lithium ion cells. *J. Power Sources* **2017**, *341*, 373–386. [[CrossRef](#)]
34. Raman, M.; Champa, V.; Prema, V. State of health estimation of lithium ion batteries using recurrent neural network and its variants. In Proceedings of the 2021 IEEE International Conference on Electronics, Computing and Communication Technologies (CONECCT), Bangalore, India, 9–11 July 2021; IEEE: Piscataway, NJ, USA, 2021.
35. Schmitt, J.; Horstkötter, I.; Bäker, B. Electrical lithium-ion battery models based on recurrent neural networks: A holistic approach. *J. Energy Storage* **2023**, *58*, 106461. [[CrossRef](#)]

Disclaimer/Publisher’s Note: The statements, opinions and data contained in all publications are solely those of the individual author(s) and contributor(s) and not of MDPI and/or the editor(s). MDPI and/or the editor(s) disclaim responsibility for any injury to people or property resulting from any ideas, methods, instructions or products referred to in the content.